

Planet formation in Alpha Centauri A revisited: not so accretion-friendly after all

P. Thébault^{1*}, F. Marzari², H. Scholl³

¹Stockholm Observatory, Albanova Universitetcentrum, SE-10691 Stockholm, Sweden, and
Observatoire de Paris, Section de Meudon, F-92195 Meudon Principal Cedex, France

²Department of Physics, University of Padova, Via Marzolo 8, 35131 Padova, Italy

³Laboratoire Cassiopée, Université de Nice Sophia Antipolis, CNRS, Observatoire de la Côte d’Azur, B.P. 4229, F-06304 Nice, France

Draft version 23 October 2021

ABSTRACT

We numerically explore planet formation around α Centauri A by focusing on the crucial planetesimals-to-embryos phase. Our approach is significantly improved with respect to the earlier work of Marzari & Scholl (2000), since our deterministic N-body code computing the relative velocities between test planetesimals handles bodies with different size. Due to this step up, we can derive the accretion vs. fragmentation trend of a planetesimal population having any given size distribution. This is a critical aspect of planet formation in binaries since the pericenter alignment of planetesimal orbits due to the gravitational perturbations of the companion star and to gas friction strongly depends on size. Contrary to Marzari & Scholl (2000), we find that, for the nominal case of a Minimum Mass Solar Nebula gas disc, the region beyond ~ 0.5 AU from the primary is strongly hostile to planetesimal accretion. In this area, impact velocities between different-size bodies are increased, by the differential orbital phasing, to values too high to allow mutual accretion. For any realistic size distribution for the planetesimal population, this accretion-inhibiting effect is the dominant collision outcome and the accretion process is halted. Results are relatively robust with respect to the profile and density of the gas disc. Except for an unrealistic almost gas-free case, the inner “accretion-safe” area never extends beyond 0.75 AU. We conclude that planet formation is very difficult in the terrestrial region around α Centauri A, unless it started from fast-formed very large (>30 km) planetesimals. Notwithstanding these unlikely initial conditions, the only possible explanation for the presence of planets around 1 AU from the star would be the hypothetical outward migration of planets formed closer to the star or a different orbital configuration in the binary’s early history. Our conclusions differ from those of several studies focusing on the later embryos-to-planets stage, confirming that the planetesimals-to-embryos phase is more affected by binary perturbations.

Key words: planetary systems: formation – stars: individual: α Centauri – planets and satellites: formation.

1 INTRODUCTION

A majority of stars are members of binary or multiple systems (e.g. Duquennoy and Mayor 1991), making the presence and frequency of planets in such systems, in particular terrestrial planets, a very relevant issue in our ongoing search for other worlds. This issue has been made all the more timely by the discovery of more than 40 extrasolar planets in multiple systems, amounting to $\sim 20\%$ of all detected exoplanets (Raghavan et al. 2006; Desidera & Barbieri 2007). Most of these planets are located in very wide binaries (> 100 AU) where the companion star’s influence at the planet’s lo-

cation is probably weak (except for possible high inclination effects between the planet’s and the binary’s orbits, see e.g. Takeda et al. 2008). However, a handful of planets, like Gliese 86, HD41004 or γ -Cephei, inhabit binaries with separations ~ 20 AU, for which the binarity of the system probably cannot be ignored.

The long term stability of planetary orbits in binaries has been explored in several studies (e.g. Holman & Wiegert 1999; David et al. 2003; Mudryk & Wu 2006), aimed at estimating a_{crit} , the distance from the primary beyond which orbits become unstable. This critical distance depends on several parameters, mainly the binary’s semi-major axis a_b and eccentricity e_b as well as the mass ratio $\mu = m_2/(m_1 + m_2)$. However, one can use as a rule of thumb that, except for extremely eccentric systems, a_{crit} is in the

* E-mail: philippe.thebault@obspm.fr

0.1-0.4 a_b range (see for example the empirical formulae derived by Holman & Wiegert 1999). As a consequence, the terrestrial planet region around 1 AU is almost always "safe" for binaries of separations > 10 AU.

The way the planet *formation* process is affected by stellar binarity is a more difficult issue. This process is indeed a complex succession of different stages¹ (e.g Lissauer 1993), each of which could react in a different way to the companion's star perturbations.

The last stage of planet formation, leading from planetary embryos to planets, has been investigated in several papers (e.g Barbieri et al. 2002; Quintana et al. 2002, 2007; Haghighipour & Raymond 2007). These studies have revealed that the (a_b, e_b, μ) parameter space for which this stage can proceed unimpeded is slightly, but not too much more limited than that for orbital stability. As an illustration, the numerical exploration of Quintana et al. (2007) showed that planetary embryos can mutually accrete at 1 AU from the primary if the companion's periastron q_2 is ≥ 5 AU.

In contrast, the stage preceding this final step, i.e. the mutual accretion of kilometre-sized planetesimals leading to the embryos themselves, is much more sensitive to binarity effects. A series of numerical studies (Marzari & Scholl 2000; Thébault et al. 2004, 2006; Paardekooper et al. 2008) have indeed shown that perturbations by the companion star can stir up encounter velocities $\langle \Delta v \rangle$ to values too high for small planetesimals to have accreting impacts. Such accretion-inhibiting configurations are obtained for a wider range of binary parameters than for the later embryo-to-planet phase. As an example, Thébault et al. (2006) (hereafter TMS06) have shown that planetesimal accretion in the 1 AU region can be perturbed in binaries with separations as large as 40 AU. These results are not surprising in themselves, and this for two reasons. 1) The growth mode in the planetesimal-accumulation phase is the so-called runaway growth, whose efficiency is very sensitive to increases of the encounter velocities (which reduce the gravitational focusing factor, e.g. TMS06). 2) It takes a much smaller perturbation to stop accretion of a 1 km body than of a lunar-sized embryo: $\langle \Delta v \rangle > 10 \text{ m.s}^{-1}$ is typically enough to achieve the former, while large embryos will hardly feel any difference in their accretion rate for such small velocity disturbances. A crucial mechanism driving the $\langle \Delta v \rangle$ evolution of the planetesimals is friction due to the primordial gas remaining in the protoplanetary disc. In a circumprietary disc, its main effect is to induce a strong phasing of neighbouring planetesimal orbits, which cancels out the large orbital parameters oscillations around the forced eccentricity e_f induced by the companion's perturbations (Marzari & Scholl 2000). A crucial point is that this effect is *size dependent*, so that while $\langle \Delta v \rangle$ between equal-sized objects are reduced, impact velocities between objects of *different sizes* are increased. TMS06 have shown that the differential phasing effect appears already for small size differences, suggesting that this effect may dominate in "real" planetesimal systems. However, the exact balance between this accretion-inhibiting effect and the accretion-friendly effect on equal-sized objects depends on the size distribution in the initial planetesimal population, a parameter which could not be thoroughly investigated in the global investigation of TMS06.

1.1 planet formation in α Centauri A

We follow here the approach of TMS06 to investigate in detail one specific system: α Centauri A. Focusing on one single system allows to take the TMS06 model a step further and explore realistic size distributions of the planetesimal population as well as crucial parameters such as gas disc density and radial profile.

At a distance of 1.33 pc, the α Cen AB binary system, with a possible third distant companion M-star Proxima (Wertheimer & Laughlin 2006), is our closest neighbour in space. α Centauri A and B are G2V and K1V stars, of masses $M_A = 1.1 M_\odot$ and $M_B = 0.93 M_\odot$ respectively. The binary's semi-major axis is $a_b = 23.4$ AU and its eccentricity $e_b = 0.52$ (Poubais et al. 2002). Holman & Wiegert (1997) have shown that the region within ~ 3 AU from the primary can harbour stable planetary orbits. However, the search for planetary companion has so far been unsuccessful. The radial velocity analysis of Endl et al. (2001) has shown that the upper limit for a planet (on a circular orbit) is $2.5 M_{\text{Jupiter}}$ around α Cen A, and this at any radius from the star. This leaves an open possibility for the presence of terrestrial planets in the crucial ~ 1 AU region.

Planet formation around α Cen A has so far been specifically investigated in 4 studies. Barbieri et al. (2002) and Quintana et al. (2002, 2007) have focused on the late embryos-to-planets stage and have found that it can proceed unimpeded in a wide inner region (≤ 2.5 AU). For the planetesimal-accretion phase, Marzari & Scholl (2000) have found that orbital phasing induced by gas drag allowed km-sized bodies to accrete in the $r \leq 2$ AU region. However, this study only considered impacts between equal-sized objects, thus implicitly overlooking the accretion-inhibiting differential phasing effect. We reinvestigate here this crucial phase, exploring in detail gas drag effects on realistic size distributions for the planetesimal population.

2 MODEL

2.1 algorithm

We use the same deterministic N-body code as in TMS06, which follows the evolution, in 3D, of a swarm of test particles submitted to the gravitational influence of both stars and to gaseous friction. This algorithm tracks all mutual encounters within the swarm and allows to derive precise statistics of the evolution of the $\langle \Delta v \rangle$ distribution. Gas drag is modelled by assuming a non evolving axisymmetric gas disc, where the only free parameter is $\rho_g(r)$, the radial profile of the gas density distribution. The drag force then reads

$$\vec{F} = -\frac{3\rho_g C_d}{8\rho_{\text{pl}} s} v \vec{v}, \quad (1)$$

where \vec{v} is the velocity of the particle with respect to the gas and v the velocity modulus. ρ_{pl} and s are the planetesimal density and physical radius, respectively. C_d is a dimensionless coefficient ≈ 0.4 for spherical bodies. Note that the planetesimal's physical size s considered for the drag computation cannot be taken for the close encounter search routine, because the collision statistics would be much too poor with the limited number of particles (typically 10^4) inherent to N-body codes. We thus have to rely on the usual prescription of assigning an inflated radius s_{num} to the particles for the encounter search routine (Thébault & Brahic 1998; Charnoz et al. 2001; Lithwick & Chiang 2007). This procedure is valid as long as it does not introduce a bias, in the form of an artificial shear component, in the $\langle \Delta v \rangle$ statistics. We take here

¹ we consider here the widely accepted "core-accretion" scenario

$s_{num} = 10^{-5}$ AU, a value which gives a precision of the order of 1 m.s^{-1} in the encounter velocity estimate ².

2.2 gas disc prescription

The axisymmetric prescription is a simplification of the real behaviour of the gas disc, which should also react to the companion star's perturbations and departs from perfectly circular streamlines (Artymowicz and Lubow 1994). To realistically model the evolution of both the planetesimal and gaseous components, using a coupled N-body and hydro approach, is an arduous task. First attempts at addressing this issue have been done by Ciecielag et al. (2007) for a simplified circular-binary case and by Paardekooper et al. (2008) for eccentric binaries. Paardekooper et al. (2008) have shown that the gas disc becomes eccentric under the companion's perturbations but that the amplitude of this eccentricity e_g depends on the choice for the numerical wave damping procedure (the flux-limiter prescription). There are two possible modes: a "quiet" low- e_g case for first order flux limiters and an "excited" high- e_g case for second order ones. In the "quiet" regime, the $\langle \Delta v \rangle$ statistics for planetesimals is relatively close to the simplified axisymmetric case. In fact for a binary of 20 AU separation, results between the two cases were indistinguishable. In the "excited" regime, encounter velocities are on average increased by a factor of ~ 2 , with respect to the circular case, for a 20 AU separation binary. It is important to point out that, regardless of the details of the wave-damping modelling procedure, the $\langle \Delta v \rangle$ are either equal to or higher than their values in the circular disc case (for a more detailed discussion, see Paardekooper et al. 2008).

Because of these uncertainties regarding the "real" behaviour of the gas disc, we chose to keep here the simplified axisymmetric gas disc approach. This choice is also motivated by the fact that these full planetesimal+gas simulations are still very CPU expensive and are thus not suited for detailed parameter-space explorations as the one which is the purpose of this study. However, in the light of the conclusions of Paardekooper et al. (2008), we think that our results should not be too different (within a factor 2 in terms of encounter velocity values) from those expected with a full N-body + Hydro modelling. In any case, a crucial point is that our results should be regarded as giving a lower boundary for the $\langle \Delta v \rangle$ estimates.

2.3 set up

We consider for each run a number $N = 10^4$ of test particles, each having the same numerical size (inflated radius) $s_{num} = 10^{-5}$ AU and physical sizes (for the gas drag computation) taken at random between two boundaries s_{min} and s_{max} . For our nominal case, we consider planetesimals in the $s_{min} = 1 \text{ km}$ to $s_{max} = 10 \text{ km}$ range. We also consider an alternative "small planetesimals" case with $s_{min} = 0.1 \text{ km}$ and $s_{max} = 1 \text{ km}$ and a "large planetesimals" case with $s_{min} = 5 \text{ km}$ and $s_{max} = 50 \text{ km}$ (see Sec.3.4). The test particles are initially distributed in an approximate terrestrial planet region, between $r_{min} = 0.3 \text{ AU}$ and $r_{max} = 1.5 \text{ AU}$. They are initially placed on almost circular orbits ($\langle e \rangle_0 \leq 10^{-5}$), so that initial encounter velocities are low enough to be in the accretion-friendly range. This choice might not correspond to a physically realistic

Table 1. Nominal case setup. The fields marked by a \checkmark are explored as free parameters in the simulations. See text for details on each parameter.

	r_{min}, r_{max}	0.3-1.5 AU
	Number of test particles	10^4
\checkmark	Physical sizes s_{min}, s_{max}	1-10 km
	Inflated radius (collision search)	10^{-5} AU
\checkmark	Gas disc radial profile	$\rho_g = \rho_{g0}(r/1\text{AU})^{-2.75}$
\checkmark	ρ_{g0}	$1.4 \times 10^{-9} \text{ g.cm}^{-3}$
	t_{final}	10^4 yrs

case, but TMS06 have shown that the initial orbital conditions are very quickly relaxed and that the system tends towards the same steady-state regardless of the initial $\langle e \rangle$ and $\langle i \rangle$.

For the gas density, we consider as a nominal case the canonical Minimum Mass Solar Nebulae (MMSN) radial profile derived by Hayashi (1981), with $\rho_g = \rho_{g0}(r/1\text{AU})^{-2.75}$ and $\rho_{g0} = 1.4 \times 10^{-9} \text{ g.cm}^{-3}$, but explore different radial profiles and ρ_{g0} values (see Sec.3.3).

The final timescale for each run is taken to be $t_{fin} = 10^4 \text{ yrs}$, i.e. the typical timescale for the runaway accretion of kilometre-sized planetesimals (e.g. Lissauer 1993). However, this choice is not too stringent, since in most cases a steady-state $\langle \Delta v \rangle$ distribution is reached in less than a few 10^3 yrs .

All characteristics of the nominal case set-up are summarised in Tab.1

2.4 $\langle \Delta v \rangle$ analysis

The distribution of encounter velocities is the main output we are interested in. For each mutual impact found by the close-encounter search routine, we record $\Delta v_{s_1, s_2}$, s_1 and s_2 being the (physical) sizes of the impacting bodies. The encounter velocity distributions are then classified in 2-D matrixes giving Δv averaged over $[s_1, s_1 + ds]$ and $[s_2, s_2 + ds]$ size intervals in the $[s_{min}, s_{max}]$ range.

The crucial issue is of course to interpret these velocities in terms of accreting or eroding impacts. For an impacting pair of sizes s_1 and s_2 , the limit between eroding and accreting impacts can be defined by the threshold velocity $v^*_{(s_1, s_2)}$. This velocity depends on several parameters obtained from energy scaling considerations. The main one is the threshold energy for catastrophic fragmentation Q^* , for which various and often conflicting estimates can be found in the literature (see Thébaud & Augereau 2007, for a thorough discussion on the subject). We follow the same conservative approach as in TMS06 and consider 2 boundary estimates for the threshold velocity, $v^*_{(s_1, s_2)low}$ and $v^*_{(s_1, s_2)high}$, derived using a weakly-resistant and strongly-resistant Q^* prescription respectively (see TMS06 for more detail). For velocities in between these 2 values, we do not draw any conclusions regarding the accretion vs. erosion balance.

Note that, despite their diversity, all prescriptions for Q^* agree that the size ranges considered here, i.e. 0.1 to 50 km, correspond to the so-called gravitational regime, where bodies' resistance is determined by gravitational binding forces. This means that Q^* is an increasing function of size. This point is crucial for the results of Sec.3.4.

² to a first order, the error in the $\langle \Delta v \rangle$ estimate is of the order of $v_{Kep}(r) \times s_{num}/r$, where r is the radial distance to the star and v_{Kep} the orbital velocity at distance r

³ although it is important to stress that cratering (i.e., non fragmenting) impacts play a crucial role in defining the accretion/erosion limit, the parameters for cratering, mainly the excavation coefficient, follow (to a first order) similar energy scaling laws as Q^*

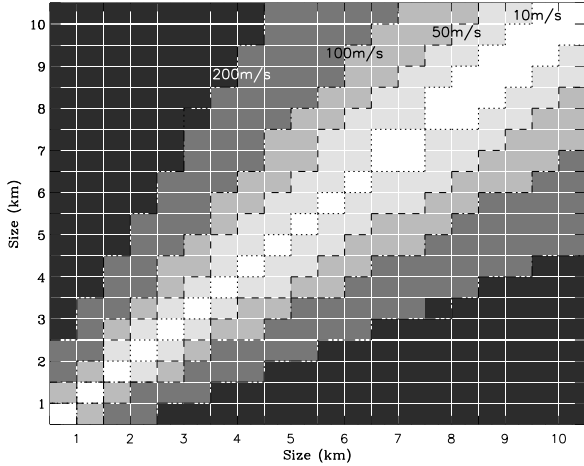


Figure 1. Mean encounter velocities $\langle \Delta v_{s_1, s_2} \rangle$, averaged in the 0.9-1.1 AU region, for all impacting pairs of sizes s_1 and s_2 in the [1, 10km] range. For the sake of clarity, 4 iso-velocity lines are represented.

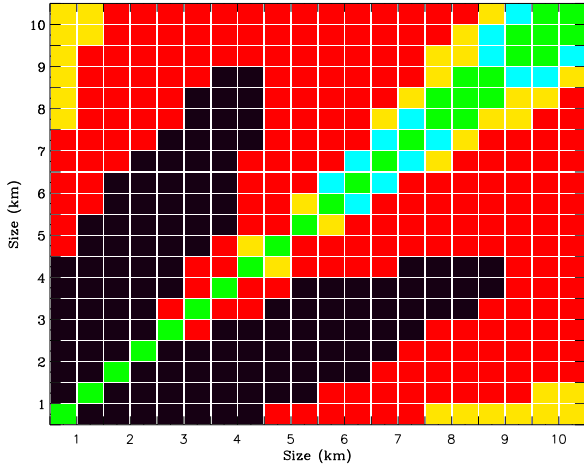


Figure 2. Same results as in Fig.1, but to each $\langle \Delta v_{s_1, s_2} \rangle$ value is associated a colour scale, depending on how this value translates into accreting or erosive impacts for each impacting pair of sizes s_1 and s_2 :

- green: no $\langle \Delta v \rangle$ variation observed, region of *unimpeded accretion*
- blue: encounter velocity increase but $\langle \Delta v \rangle \leq v_{*low}$, *perturbed accretion with slow-down of the runaway growth*
- yellow: $v_{*low} \leq \langle \Delta v \rangle \leq v_{*high}$, *uncertain accretion vs. erosion balance*
- red: $\langle \Delta v \rangle \geq v_{*high}$, *erosion*
- black: $\langle \Delta v \rangle \geq 2 \times v_{*high}$, *erosion*

3 RESULTS

3.1 $\langle \Delta v \rangle$ distribution, erosion threshold

Fig.1 shows the $\langle \Delta v_{s_1, s_2} \rangle$ distribution, at 1 AU from the primary and for bodies in the [1, 10km] range, once a steady-state is reached, i.e. after $\approx 3 \times 10^3$ yrs. The sharp size dependence of encounter velocities is here clearly visible. Low $\langle \Delta v \rangle$ are restricted to a narrow stripe along the $s_1 = s_2$ diagonal, corresponding to the domain where gas drag aligns orbits towards the same value. However, for any small departure from the exact $s_1 = s_2$ condition, encounter velocities dramatically increase. We get $\langle \Delta v_{s_1, s_2} \rangle \geq 50 \text{m.s}^{-1}$ in almost

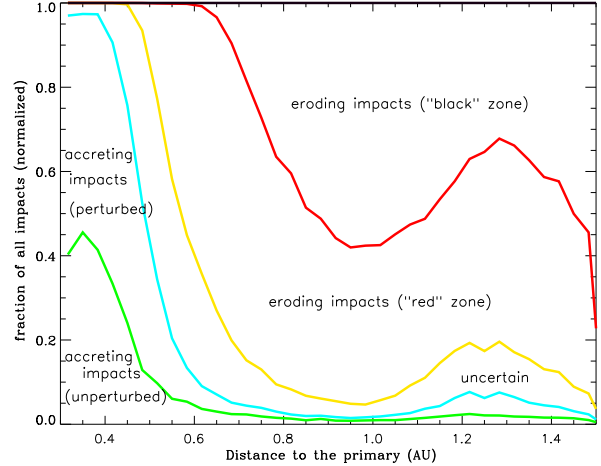


Figure 3. Relative importance of different types of collision outcomes (corresponding to the different colour categories of Fig.2), as a function of distance to the primary star. All close encounters between all bodies in the $[s_{min}, s_{max}]$ size range are taken into account, with each close encounter weighted assuming that the size distribution for the planetesimals follows a Maxwellian distribution centered on 5km (see text for details).

the whole $s_1 \neq s_2$ region. This illustrates very clearly the strength of the differential orbital phasing mechanism.

Fig.2 shows how these velocities can be interpreted in terms of accreting/erosive impacts. The only region where encounter velocities are low enough for the accretion process to proceed unimpeded (in green) is the narrow $s_1 = s_2$ diagonal. This diagonal is surrounded, for objects >5 km, by an equally narrow band (in light blue) where $\langle \Delta v \rangle$ allow accretion ($\langle \Delta v \rangle_{s_1, s_2} \leq v_{*(s_1, s_2)low}$) but are nevertheless increased with respect to their initial unperturbed value. This means that the accretion rate is slowed down, compared to the unperturbed case, since the runaway growth mode's efficiency decreases with increasing encounter velocities. Except for a small region (in yellow) of uncertain accretion/erosion balance where $v_{*(s_1, s_2)low} \leq \langle \Delta v \rangle_{s_1, s_2} \leq v_{*(s_1, s_2)high}$, all other (s_1, s_2) encounters result in eroding impacts. In these red and black areas, which cover most of the graph, velocities exceed $v_{*(s_1, s_2)high}$, our most conservative estimate for the threshold velocity .

3.2 accreting vs eroding impacts: size distribution

Of course, Fig.2 cannot in itself give the relative importance of the accreting-friendly vs. accretion-hostile areas. To do so, the real *size distribution* of the planetesimals should be known, whereas in the runs all sizes were chosen at random between s_{min} and s_{max} . The size distribution of a typical initial planetesimal population is a complex issue, which is directly linked to the very difficult (and yet unresolved) problem of the mechanisms for planetesimal formation. This problem exceeds by far the scope of the present paper (see, however, the discussion in TMS06 and in the last Section of the present paper). In line with our conservative approach, we shall here assume a fiducial size distribution which is *a priori* favourable to same-size impacts (that is, to accretion), i.e. a Maxwellian $f_{mx}(s)$ peaking at a median value $s_{med} = 5$ km. ⁴ We then weight each

⁴ Some planetesimal-accumulation particle-in-a-box models make the assumption of a single-size initial population (e.g. Weidenschilling et al.

(s_1, s_2) impact by $f_i = f_{mx}(s_1) \times f_{mx}(s_2)$, the (normalised) probability of such an impact with a $f_{mx}(s)$ size distribution. Depending on $\langle \Delta v \rangle_{s_1, s_2}$, all impacts are then classified into one of the 5 collision-outcome categories defined earlier (see Fig.2), where their contribution is weighed by f_i . Comparing the total Σf_i for each category then gives the relative importance of each of these possible collision outcomes.

As can be seen in Fig.3, at 1 AU less than 2% of all impacts result in accretion (a value which only increases to $\sim 5\%$ when including the "uncertain-outcome" category), while 95% should lead to net erosion of the impacting bodies. The dynamical environment is thus globally very hostile to accretion. Fig.3 also shows that this accretion-hostile environment extends over most of the system. Only the innermost $r \leq 0.5$ AU region has a favourable accretion vs. erosion balance. This accretion-friendly inner zone is mostly due to weaker gravitational perturbations by the companion star.

Between 1.2 and 1.4 AU, a slight increase in the accreting/eroding impacts ratio is observed, which is mostly due to weaker gas drag-induced differential phasing. However, even there the fraction of impacts with $\langle \Delta v \rangle \leq v_{*low}$ never exceeds 8%. Moreover, beyond 1.4 AU, accreting impacts quickly decrease to 0 again. The reason for high $\langle \Delta v \rangle$ in these outermost regions is no longer gas friction but pure gravitational effects. Indeed, although in the absence of gas drag the companion star forces secular orbital oscillations around e_f which should in principle not induce high $\langle \Delta v \rangle$ because they preserve the same phasing for all bodies (regardless of their size), these oscillations get narrower with time and at some point orbital crossing occurs, leading to an abrupt relative velocity increase (for a more detailed description of this effect, see section 2 of TMS06). Strong gas drag can prevent this crossing from happening, by cancelling out the oscillations and inducing it's own size-dependent phasing, but in the outer regions it is too weak to do so. In other words, planetesimals are here caught between a rock and a hard place:

- In the outer regions, pure gravitational perturbations lead to orbital crossing and high $\langle \Delta v \rangle$
- In the inner regions, gas drag can prevent orbital crossing but induces size-dependent orbital phasing which also leads to high $\langle \Delta v \rangle$

We have tested the robustness of our results with respect to different choices of the size distribution. Collisional-"equilibrium" power laws with $dN \propto s^{-3.5} ds$ and Gaussians centred on s_{med} of various widths have been considered. Although some differences were observed with respect to our nominal case, they remain relatively marginal and our main conclusions seem to hold regardless of the size distribution (see Fig.4). This is true in particular for the region around 1 AU which is always strongly hostile to accretion: the fraction of accreting impacts never exceeds 10% for all tested size distributions. The only case giving an accretion-friendly environment is an almost Dirac-like Gaussian of variance $(0.25 \text{ km})^2$, but this size distribution is probably highly unrealistic. Another important robust result is that there is always an inner region having low $\langle \Delta v \rangle$ enabling accretion. The outer edge of this inner zone varies slightly with the size distribution prescription, but is always located in the 0.5 – 0.6 AU range.

1997), but this is of course a numerically convenient simplification which cannot correspond to a "real" population which necessarily has a spread in sizes

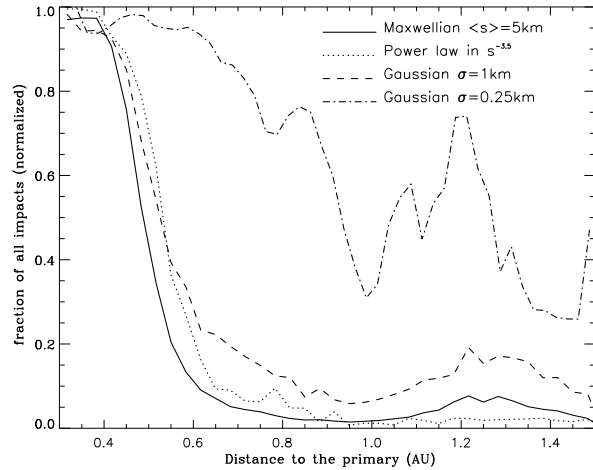


Figure 4. Fraction of accreting impacts (limit between the "blue" and "yellow" zones) for different prescriptions for the size distribution. The noisiness of the curve corresponding to the extremely narrow-Gaussian is due to the fact that in this case only impacts for a very narrow $s_1 \sim s_2$ region have non-negligible weigh in the global statistics.

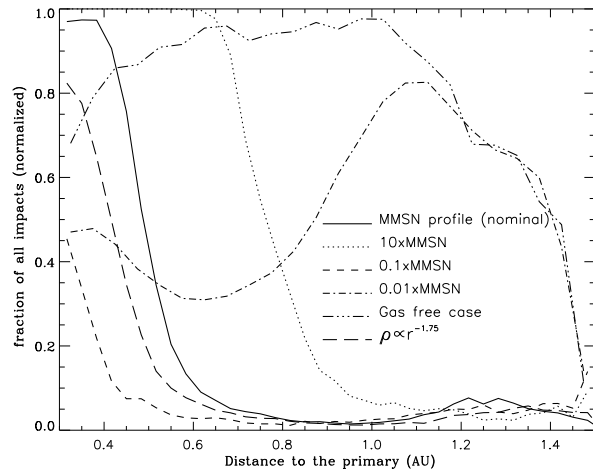


Figure 5. Fraction of accreting impacts (limit between the "blue" and "yellow" zones) for different prescriptions for the gas disc (see text for details).

3.3 Different gas disc profiles

For our nominal case, we assumed a standard MMSN gas disc, but other gas disc models have been explored (Fig.5).

We first consider the same $\rho_g = \rho_{g0}(r/1\text{AU})^{-2.75}$ profile as in the nominal case but with a different reference value for ρ_{g0} at 1 AU chosen around the MMSN $\rho_{g0(ref)} = 1.4 \times 10^{-9} \text{ g.cm}^{-3}$ value.

As it can be seen, for larger values of ρ_{g0} the situation becomes slightly more favourable to accretion, and the outer edge of the inner accretion-friendly zone moves to ~ 0.75 AU for the highest $\rho_{g0} = 10 \times \rho_{g0(ref)}$ explored value. This is due to the fact that complete differential phasing, meaning that objects of all sizes reach steady-state eccentricity and periastron longitude ω values before t_{final} , is already achieved for the nominal MMSN case. Thus, when increasing the gas density, no "better" phasing is achieved. The effect of increased ρ_g is then that all steady-state e and ω values globally tend towards their asymptotic value for infinitely small

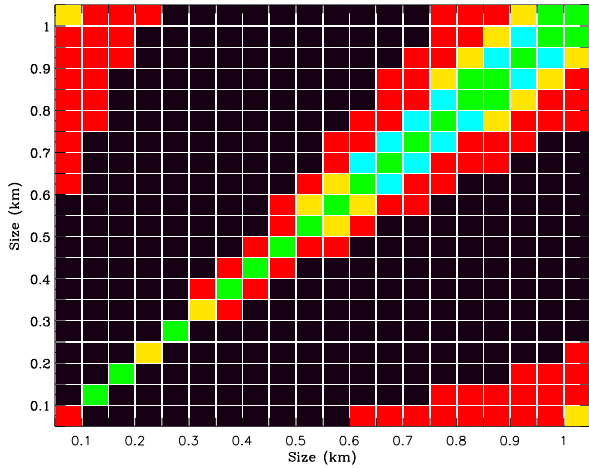


Figure 6. Same as Fig.2, but for the "small planetesimals" run. The colour scaling for the different accretion/erosion zones is the same as in Fig.2.

sizes, i.e. $e = 0$ and $\omega = 270^\circ$ (see Eqs.24-29 of Paardekooper et al. 2008), which tend to reduce encounter velocities.

The effect of decreasing gas densities is more complex to interpret. For ρ_{g0} just below $\rho_{g0(\text{ref})}$, relatively good differential phasing is maintained but all steady-state e and ω values globally move away from their asymptotic $s \rightarrow 0$ value. This results in a wider spread of steady-state orbital parameters and thus higher $\langle \Delta v \rangle$. Below a threshold value ($\sim 0.1 \times \text{MMSN}$), however, steady state phasing is no longer achieved for the biggest bodies, which then still have substantial e and ω oscillations after t_{final} . Since phasing is still achieved for the smallest objects, the *difference* between the orbits of small and big bodies is still increasing. This is what is clearly observed for the $\rho_{g0} = 0.1 \rho_{g0(\text{ref})}$ run. However, below a second threshold value ($\sim 0.01 \times \text{MMSN}$), steady state phasing breaks down for *all* bodies. The system now moves towards its gas-free behaviour, with large common orbital oscillations for all bodies, and high $\langle \Delta v \rangle$ only in the regions where oscillations are narrow enough for orbital crossing to occur, i.e. beyond $\sim 1.3 \text{ AU}$ (see discussion in the previous section).

We finally consider a case with a different radial dependence for the gas density, i.e. a flatter profile in $\rho_g = \rho_{g0}(r/1\text{AU})^{-1.75}$ (ρ_{g0} being the same as in the nominal case). The accretion/erosion balance is slightly less favourable than in the nominal MMSN case, with the outer edge of the inner "safe" zone at $\sim 0.45 \text{ AU}$ (dashed curved in Fig.5).

However, despite all these quantitative differences, the qualitative results remain relatively similar for all test gas disc cases, with the exception of the probably unrealistic very-gas-poor runs. The generic characteristics are an inner accretion-friendly zone, whose outer edge varies from 0.35 to 0.75 AU, followed by a vast region where impacts are predominantly erosive for all objects in the 1-10 km range. More importantly, the crucial region for habitable planets around 1 AU is always in an environment hostile to accretion.

3.4 Alternative planetesimal size-ranges

We have so far assumed a planetesimal population in the 1-10 km size range, which corresponds to the most generic choice for an "initial" planetesimal population (see e.g. Greenberg et al. 1978;

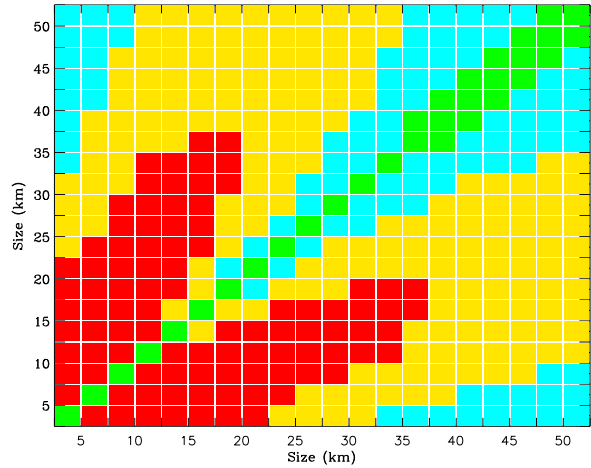


Figure 7. Same as Fig.2, but for the "large planetesimals" run. The colour scaling for the different accretion/erosion zones is the same as in Fig.2.

Wetherill & Stewart 1989; Barge & Pellat 1993; Lissauer 1993; Weidenschilling et al. 1997). However, because the planetesimal-formation phase is still poorly understood (see for example Youdin & Chiang (2004) and Cuzzi & Weidenschilling (2006) for conflicting views on the matter), this few-km size range is far from being a value carved in marble. Two other possible initial size ranges, with $0.1 \leq s \leq 1 \text{ km}$ and $5 \leq s \leq 50 \text{ km}$, have thus been explored in our simulations. Note that if from a purely dynamical point of view changing the planetesimal sizes is equivalent to changing the gas density (because of the $1/s$ dependence of the gas drag force), it is not equivalent from the point of view of the accretion/erosion behaviour. As an example, an impact between a 1 km and a 5 km body in a gas disc of density ρ_g occurs on average at the same velocity $\langle \Delta v \rangle_{1,2}$ as an impact between a 10 km and 50 km body in a $10 \times \rho_g$ disc, but the outcome of a $\langle \Delta v \rangle_{1,2}$ collision between 1 km and 5 km objects will not be the same as for 10 km and 50 km objects

For our "small" planetesimals population in the 0.1-1 km range, we obtain, not surprisingly, a situation which is more hostile to accretion (Fig.6). This is not due to higher relative velocities than in the nominal case, since $\langle \Delta v \rangle_{1,2}$ are of the same order than in the 1-10 km run. The explanation is to be found in the fact that such small objects are much more affected by $\langle \Delta v \rangle$ increase, and this for 2 reasons: 1) They have lower threshold Q^* values, and 2) they have lower escape velocities.

For the "large" planetesimals run with $s_{\text{min}} = 5 \text{ km}$ and $s_{\text{max}} = 50 \text{ km}$, on the contrary, we find an environment which is more favourable to accretion than in the nominal case (Fig.7). The accretion-friendly zone now covers a large fraction of the (s_1, s_2) phase space at 1 AU, especially in the $\geq 30 \text{ km}$ range. As for the small planetesimals case, this result is only marginally due to lower relative velocities, since the distribution of $\langle \Delta v \rangle_{1,2}$ is here again close to that of the nominal case. What makes a difference here is that bodies in the 10-50 km range are much more resistant to impacts than smaller ones. They are also big enough to reaccumulate a substantial fraction of the mass they might lose after an impact (a process which is taken into account in our estimate of $v^*_{(s_1, s_2)\text{low}}$ and $v^*_{(s_1, s_2)\text{high}}$).

4 DISCUSSION AND CONCLUSIONS

Our numerical exploration has shown that for our nominal case set-up the $r \geq 0.5$ AU region around α Centauri is hostile to kilometre-sized planetesimal accretion. The coupling of the companion star's secular perturbations with the size-dependent phasing imposed by gas drag leads to high $\langle \Delta v \rangle_{(s_1, s_2)}$ destructive collisions for all $s_1 \neq s_2$ pairs. For any realistic size distribution for the planetesimal population (except very unlikely Dirac-like size distributions), these erosive impacts outnumber by far the low-velocity $s_1 \sim s_2$ encounters and are the dominant collision outcome. Only the innermost region within ~ 0.5 AU has $\langle \Delta v \rangle$ low enough to allow planetesimal accretion.

Interestingly, these results are relatively robust when varying the gas disc density. The main difference is that the outer limit of the inner "accretion-safe" region varies between 0.35 and 0.75 AU. Only for very gas poor systems do we get a qualitatively different behaviour, with the safe region extending up to ~ 1.3 AU, where a high- $\langle \Delta v \rangle$ zone due to pure secular perturbations begins.

These results are further strengthened by the fact that our simplified assumption for the gas disc probably results in a slight underestimate of $\langle \Delta v \rangle_{(s_1, s_2)}$ values (see discussion in Sec.2.2). As a consequence, our approach can be regarded as conservative regarding the extent of the impact velocity increase which is reached, the "real" system being probably even more accretion-hostile than in the presented results.

This hostility to kilometre-size planetesimal accretion is of course a major threat to planet formation as a whole, of which it is a crucial stage. However, before reaching any definitive conclusions, one has to see if there might be some ways for planetary formation to get round this hurdle. In the next 3 subsections we critically examine three such possibilities.

4.1 Accretion from large initial planetesimals?

We have seen that, apart from an unrealistic gas-free case, the only way to get an accretion friendly environment at 1 AU is to assume large, ≥ 30 km planetesimals which can sustain the high velocity regime without being preferentially eroded (Fig.7). This solution to the high velocity problem raises however important issues. One of them is how realistic it is to assume a population of large initial planetesimals. As already pointed out, the planetesimal formation process is still too poorly understood to reach any definitive conclusion regarding what an initial planetesimal population looks like, so that values in the 30-50 km range cannot be ruled out *a priori*. Nevertheless, one has to ask the question of what was *before* these large planetesimals. Should these objects arise from the progressive accumulation of grains, rocks and pebbles in a turbulent nebula (as in the standard coagulation model, e.g. Dullemond & Dominik 2005), then there is no clear cut separation between the planetesimal-formation phase and the subsequent planetesimal-to-embryo phase⁵. In this case, the stage where the biggest planetesimals are ~ 50 km in size should be preceded by a stage where the biggest objects are in the 1-10 km range, which leads us back to the accretion-inhibiting nominal case. The only solution would be to bypass these intermediate accretion-inhibiting stages by directly forming large planetesimals. This could in principle be achieved with the alternative gravitational instability scenario (e.g. Goldreich & Ward 1973;

Youdin & Chiang 2004), but this scenario still has several problems to overcome (see for instance Armitage 2007, for a brief review). Moreover, it is not clear how gravitational instabilities should proceed in the highly perturbed environment of a binary.

It should also be noted that even *if* at some point this accretion-friendly large-planetesimals stage is reached, the way accretion will proceed from there would be very different from the standard runaway-accretion scheme. Indeed, as can be clearly seen in Fig.7, the (s_1, s_2) parameter space for which accretion can proceed unimpeded is restricted to a narrow $s_1 \sim s_2$ band. For most impacts on $s \geq 30$ km targets, even if relative velocities are below $v_{*(s_1, s_2)low}$ (the "blue" zone), they are nevertheless increased relative to the unperturbed case. These increased $\langle \Delta v \rangle$ would strongly reduce the gravitational focusing factor which is the key process driving runaway accretion. In this case, the growth mode could be the so-called "type II" runaway identified by Kortenkamp et al. (2001), corresponding to a slowed-down runaway growth in a high $\langle \Delta v \rangle$ environment.

4.2 Accretion once gas has dissipated?

An interesting issue is what happens *after* gas dispersal. Indeed, it is believed that primordial gas discs dissipate, due to photo-evaporation and/or viscous accretion onto the central star, in a few 10^6 years (e.g. Alexander et al. 2006), a timescale which could even be shortened in binaries because of the outer truncation of the protoplanetary disc. One might thus wonder if, despite of a long accretion-hostile period while gas is present, planetesimal accretion could start anew once the environment becomes gas free and differential phasing effects disappear. However, for this to occur, there is a big difficulty to overcome. Indeed, when the environment becomes gas free, all planetesimals are still on the differentially-phased orbits they were forced onto by gas friction. This means that the *initial* dynamical conditions are such as $\langle \Delta v \rangle_{(s_1, s_2)}$ are high. Under the sole influence of the companion star's secular perturbations (the only external force left in the gas free system), these initial orbital differences cannot be erased or damped. The size-independent orbital phasing which will be forced by secular effects will come *in addition* to the initial orbital differences, which can in this respect be regarded as an initial free component. This behaviour can be easily checked by gas free test simulations.

Moreover, even if a hypothetical additional mechanism acts to damp the initial differential phasing, it has to act quickly in order to lead to low impact velocities. Indeed, if given enough time, secular perturbations *alone* will eventually induce high $\langle \Delta v \rangle$ due to orbital crossing of neighbouring orbits. The inner limit of ~ 1.3 AU for such orbital crossing given in Sec. 3.2 is indeed the one reached at $t = 10^4$ yrs, but this limit is moving inwards with time. Using the empirical analytical expressions derived by TMS06 (see Eq.15 of that paper), we find that the orbital crossing "front" reaches the 0.5 AU region after $\sim 1.5 \times 10^5$ yrs.

As a consequence, it seems unlikely that $\langle \Delta v \rangle_{(s_1, s_2)}$ can be significantly reduced in the later gas free system. Collisional erosion, started in the gas-rich initial disc, should thus probably continue once the gas has dissipated⁶.

⁵ In this case, the very concept of an "initial" planetesimal population might be questioned (see for instance Wetherill & Inaba 2000)

⁶ As this paper was being reviewed, a yet unpublished study by Xie and Zhou (ApJ, submitted, with a preliminary summary in Xie & Zhou 2008) was brought to our attention. It explores the possibility, for the specific case of γ Cephei and under possibly extreme assumptions for gas dispersal

4.3 Outward planet migration and different initial binary configuration

It could be argued that planets could have formed elsewhere and later migrated to the $r \geq 0.75$ AU regions (the maximum extent of the accretion-friendly region obtained in our gas-disc profile exploration). Early migration of the protoplanets by interaction with the primordial gas disc might be ruled out since such a migration (be it of type I, II or III, e.g. Papaloizou et al. 2007) would be inwards. In the present case, the planets would thus have to come from further out in the disc, i.e. from regions which are even more hostile to accretion. Outward drift of planets could however occur for another type of migration, the one triggered, after gas-disc dispersal, by interactions between a multi-planets system and a massive disc of remaining planetesimals (as in the so-called Nice-model, e.g. Tsiganis et al. 2005). Nevertheless, it remains to see how this scenario, which was studied for mutually interacting giant planets at radial distances between 5 and 30 AU, would work in the present case, ~ 10 times closer to the star and with probably much less massive planets. This important issue will be addressed in a forthcoming paper (Scholl et al., in preparation).

An alternative possibility would be that the binary's orbital configuration was not the same in the past as it appears today. If the presently observed binary system was part of an unstable multiple system (triple or more), planets might have formed when the binary had a larger semi-major axis and it was less eccentric (Marzari & Barbieri 2007). Both these conditions could lead to a more favourable environment for planetesimal accretion than present. In this scenario planets should have formed prior to the onset of the stellar chaotic phase which inevitably ends with the ejection of one star, leaving the remaining binary system with smaller separation and higher eccentricity. The discussion of the possible consequences of a transient triple system stage for α Centauri A and B is complicated by the presence of Proxima Cen, a red dwarf located roughly a fifth of a light-year from the AB binary. A recent paper by Wertheimer & Laughlin (2006) argues that the binding energy of Proxima Centauri relative to the centre of mass of the α Centauri binary is indeed negative, even if the star is close to the outer border of the Hill's sphere of the AB system in the galactic potential. This might be an indication of a violent past of the system when the AB binary was possibly part of a higher multiplicity unstable stellar system. This issue exceeds the scope of the present paper and should be explored in future studies.

4.4 Conclusion and Perspectives

Because of the hypothetical additional effects listed in Sec.4.3, the presence of planets beyond 0.75 AU cannot be fully ruled out. However, we think that our results on planet formation, with the present binary configuration, are relatively robust. Our main result is that it is very difficult for $s \leq 30$ km planetesimals to have accreting encounters beyond 0.5-0.75 AU from the primary, which makes planet formation very unlikely in these regions. These results are in sharp contrast to those of Marzari & Scholl (2000), who found the terrestrial region around α Centauri A to be favourable to planetesimal accumulation. The main reason for this discrepancy is that Marzari & Scholl (2000) restricted their pioneering study

to collisions between *equal-size* bodies, for which gas friction indeed decreases $\langle \Delta v \rangle$ and favours accretion, thus implicitly neglecting the dominant effect of eroding $s_1 \neq s_2$ impacts. Our results are also in contrast to the conclusions of Barbieri et al. (2002) and Quintana et al. (2002, 2007), who regarded planet accretion as been possible in the inner ≤ 2.5 AU region. This is because these studies focused on the later embryo-to-planet phase, thus implicitly assuming that the preceding planetesimal-to-embryo phase was successful. The present study shows that this is probably not the case. This confirms that the planetesimals-to-embryos phase is more affected by the binary environment than the last stages of planet formation.

Due to the complexity of the coupling between secular perturbations and gas drag, and their strong dependence on binary orbital elements, the present results cannot be directly extrapolated to other systems. Clearly, such detailed studies of planetesimal accumulation in other close binary systems, either those known to harbour planets (like γ Cephei⁷ or HD41004) or those being potential candidates, should be undertaken in the close future. In this respect, one object of particular interest could be α Cen A's companion, Alpha Centauri B, for which Guedes et al. (2008) very recently explored the possibilities for observational detection of terrestrial planets.

REFERENCES

- Alexander, R. D., Clarke, C. J., Pringle, J. E., 2006, MNRAS, 369, 229
- Armitage, Philip J., Lecture notes on the formation and early evolution of planetary systems, 2007, arXiv:astro-ph/0701485
- Artymowicz, P., Lubow, Stephen H., 1994, ApJ, 421, 651
- Barbieri, M.; Marzari, F.; Scholl, H., 2002, A&A, 396, 219
- Barge, P., Pellat, R., 1993, Icarus, 104, 79
- Charnoz, S.; Thébault, P.; Brahic, A., 2001, A&A, 373, 683
- Ciecielag, P.; Ida, S.; Gawryszczak, A.; Burkert, A., 2007, A&A, 470, 367
- Cuzzi, J., Weidenschilling, S., Particle-Gas Dynamics and Primary Accretion, 2006, in Meteorites and the Early Solar System II, D. S. Lauretta and H. Y. McSween Jr. (eds.), University of Arizona Press, Tucson, 943 pp., p.353-381
- David, E., Quintana, E. V., Fatuzzo, M., Adams, F. C., 2003, PASP, 115, 825
- Desidera, S., Barbieri, M., 2007, A&A 462, 345-353
- Dohnanyi J.S., 1969, JGR 74, 2531
- Dullemond, C., Dominik, C., 2005, A&A, 434, 971
- Duquennoy, A.; Mayor, M., 1991, A&A, 248, 485
- Endl, M.; Kurster, M.; Els, S.; Hatzes, A. P.; Cochran, W. D., 2001, A&A, 374, 675
- Goldreich, P., Ward, W., 1973, ApJ, 183, 1051
- Greenberg, R.; Hartmann, W. K.; Chapman, C. R.; Wacker, J. F., 1978, Icarus, 35, 1
- Guedes, J. M.; Rivera, E. J.; Davis, E.; Laughlin, G.; Quintana, E.V.; Fischer, D.A., 2008, ApJ, in press, arXiv:astro-ph/08023482
- Haghighipour, N., & Raymond, S. N. 2007, ApJ, 666, 436
- Hayashi, C., 1981, PthPS 70, 35
- Holman, M.J., Wiegert, P. A. 1997, AJ, 113, 1445
- Holman, M.J., Wiegert, P. A. 1999, AJ, 117, 621

timescales, that some "re-phasing" might occur *during* the gas dissipation phase

⁷ γ Cephei has already been investigated by Thébault et al. (2004), but with a simplified version of the present code, in particular with respect to the role of planetesimal size distributions

- Kortenkamp, S., Wetherill, G., Inaba, S., 2001, *Science*, 293, 1127
- Lissauer, J.J., 1993, *ARA&A* 31, 129
- Lithwick, Yoram; Chiang, Eugene, *Collisional Particle Disks*, 2007, *ApJ*, 656, 524
- Marzari F., Scholl H., 2000, *ApJ* 543, 328
- Marzari, F. and Barbieri, M. 2007, *A&A*, 467, 347-351
- Mudryk, Lawrence R.; Wu, Yanqin, 2006, *ApJ*, 639, 423
- Paardekooper, S.-J., Thébault, P., Mellema, G. 2008, *MNRAS*, 386, 973
- Papaloizou, J. C. B.; Nelson, R. P.; Kley, W.; Masset, F. S.; Arty-mowicz, P., in "Protostars and Planets V", B. Reipurth, D. Jewitt, and K. Keil (eds.), University of Arizona Press, Tucson, 951 pp., 2007., p.655-668
- Pourbaix, D.; et al., 2002, *A&A*, 386, 280
- Quintana, E. V., Lissauer, Jack J.; Chambers, John E.; Duncan, Martin J., 2002, *ApJ*, 576, 982
- Quintana, E. V., Adams, F. C., Lissauer, J. J., & Chambers, J. E. 2007, *ApJ*, 660, 807
- Raghavan, Deepak; Henry, Todd J.; Mason, Brian D.; Subasavage, John P.; Jao, Wei-Chun; Beaulieu, Thom D.; Hambly, Nigel C., 2006, *ApJ*, 646, 523
- Takeda, G, Kita R., Rasio F.A., 2008, *ApJ*, submitted, arXiv:0802.4088
- Thébault, P., Brahic, A. 1998, *P&SS*, 47, 233
- Thébault, P., Marzari, F., Scholl, H., Turrini, D., Barbieri, M., 2004, *A&A*, 427, 1097
- Thébault, P., Marzari, F., Scholl, H., 2006, *Icarus*, 183, 193
- Thébault, P., Augereau J.-C., 2007, *A&A*, 472, 169
- Tsiganis, K.; Gomes, R.; Morbidelli, A.; Levison, H. F., 2005, *Nature*, 435, 459
- Weidenschilling S.J., Spaute D., Davis D.R., Marzari F., Ohtsuki K., 1997, *Icarus* 128, 429.
- Wertheimer, J.G., and Laughlin, G., 2006, *AJ*, 132, 1995
- Wetherill, G.W., Stewart, G.R., 1989, *Icarus*, 77, 330
- Wetherill, G.W., Inaba, S., 2000, *SSRv*, 92, 311
- Xie, Ji-Wei; Zhou, Ji-Lin, 2008, in "Exoplanets: Detection, Formation and Dynamics, Proceedings of the International Astronomical Union, IAU Symposium", Volume 249, 419-424
- Youdin, A., Chiang, E., 2004, *ApJ*, 601, 1109